Available online at www.sciencedirect.com
SCIENCE DIRECT®
Journal of Food Engineering 76 (2006) 506–523
JOURNAL OF FOOD ENGINEERING
www.elsevier.com/locate/jfoodeng

Discrimination and classification of fresh-cut starfruits (*Averrhoa carambola* L.) using automated machine vision system

M.Z. Abdullah [a,*], J. Mohamad-Saleh [a], A.S. Fathinul-Syahir [a], B.M.N. Mohd-Azemi [b]

[a] *School of Electrical and Electronic Engineering, Engineering Campus, University Science Malaysia, 14300 Penang, Malaysia*
[b] *School of Industrial and Food Technology, University Science Malaysia, 18000 Penang, Malaysia*

Received 19 October 2004; accepted 21 May 2005
Available online 28 July 2005

Abstract

Software for detecting the quality features of golden delicious starfruits of *Averrhoa carambola* L. genus were developed for automated inspection system using machine vision technology. The features considered were colour and shape. The use of artificial classifiers such as linear discrimination analysis and multi-layer perceptron neural network as a tool to detect starfruit maturities such as unripe, underripe, ripe and overripe in HSI colour space were investigated. The colour spectra of matured and unmatured fruits were characterised using all colour features ranging from hue 10 to hue 74, and, using principal hues generated by Wilks-lambda analysis. Experiments performed on 200 independent starfruit samples revealed that linear discriminant analysis after Wilks-lambda analysis was more precise in classification than direct application of linear discriminant analysis. However, the classification accuracy of multi-layer preceptron remained relatively the same before and after feature reduction. Overall, the average correct classification for linear discriminant analysis and multi-layer preceptron was 95.3% and 90.5% respectively during testing stage. Meanwhile the use of Fourier transform was investigated for shape discrimination. This algorithm produced 100% success rate in detecting starfruits by three shape categories: well-formed, slightly deformed and seriously deformed. Both colour and shape analysis was easily affected by the variation of lighting levels, and this contributed to the major classification error.

Keywords: Linear discriminant analysis; Multi-layer preceptron; Neural networks; Machine vision; Starfruit grading; Automated quality inspection

1. Introduction

Among the many quality tests that need to be carried out on fresh-cut starfruits (*Averrhoa carambola* L.) during processing and packaging processes are the measurement of colour and shape. Consumers consider good quality fruits to be those that look good, are firm and offer good flavour and nutritive value. Like any other ordinary tropical fruits, colour is very important attribute in starfruits since colour indicates maturity and ripeness. Colour change is the most conspicuous aspect of ripening and, consciously or unconsciously, this is the aspect most used in selecting starfruits either for harvest or consumption. In this respect, degreening is the most clear indication of ageing and decreasing freshness of starfruits besides loss of tugor and decay. In a study on the process of ripening of starfruits, the changes in colours have been associated with firmness, cellulose, hemicellulose and pectin contents and reported that the colour represents an accurate means to determine the fruit ripeness (Mitcham & McDonald, 1991). Colour is not only measured solely to ascertain starfruit aesthetic quality, but is also used as a guide to more practical matters such as the determination of storage-life and best-if-used-by-date. The capability of the fruit for storage at longer periods without comprising its quality and its ability to ripen normally at 23 °C, can be

* Corresponding author. Tel.: +60 4 5937788; fax: +60 4 5941023.
E-mail address: mza@usm.my (M.Z. Abdullah).

0260-8774/$ - see front matter © 2005 Elsevier Ltd. All rights reserved.
doi:10.1016/j.jfoodeng.2005.05.053

programmed to supply fruits of required maturity such as green mature, half ripe or full ripe, to the consumers as well as to the fruit processing industries. In this regard, immature fruits are more subject to shrivelling and mechanical damage and are of inferior quality when ripe. Overripe fruits, on the other hand, are likely to become soft and mealy insipid flavour soon after harvest. Any fruit picked either too early or too late in its season is more susceptible to physiological disorders and has shorter storage-life than fruit picked at the proper maturity (Kader, 1999). Unfortunately, maturity is an ambiguous term in starfruit crop horticulture. This ambiguity partially arises from the difficulty in measuring and quantifying colour in a more objective manner. The problem is further complicated due to a non-uniform ripening nature of starfruits, causing irregularities and inconsistencies in ripeness judgements. Previous study has indicated that although starfruit trees can produce total yields of 20 kg, increasing up to 500 kg per tree when the tree matures in 6–7 years, nearly 90% of the fruits can be rejected due to inefficient postharvest processing (Nakasone & Paull, 1998).

As consumers also consider good quality starfruits to be those that look uniform, in addition to colour, shape is also important quality attribute of starfruits. The ordinary and oxalidaceae family type starfruits resemble an elongated Chinese lantern, may be up to 5–12 cm long, 3–6 cm across, with typically five strongly pointed ridges or deep flutings that run from top to the bottom. Consequently, when the fruit is cut crosswise each slice is uniquely shaped like a star having five corners or five fingers. However, within each fruit species there is a range of genotypic variation in shape quality, resulting primarily from the effects of preharvest climatic conditions and cultural practices, variability between seasons, orchards and cultivars (Lee & Kader, 2000). Therefore and in addition to common 5-angled starfruits, there are also 4-angled and 6-angled starfruits. The formation of 6-angled star shape is quite common but rare for 4-angled star shape. Defects originating before harvest and as a result of damage by insects, diseases, birds, chemical injuries, and various blemishes such as scars, scabs, russeting and rind staining add more kinds of shapes. Expectedly, the removal of starfruits with undesirable appearances will improve their overall quality and thus, minimising postharvest losses. The producers and handlers are concerned with appearance along with long postharvest life because buyers and consumers are willing to pay higher price for picking maturities that are superior in quality and fruits that appear homogeneous. Moreover, the producers and handlers are interested to salvage starfruits of inferior and inconsistent qualities for use in jelly making or drink processing which otherwise rejected by the consumers. Therefore, grading is an integral and important procedures for harvesting, storing, marketing and processing of starfruits.

Presently the inspection and grading of starfruits are carried out by human inspectors who make quality assessment by "seeing" and "feeling" for a particular quality attribute. In addition to being costly, this method is highly variable and decisions are not always consistent between inspectors or from day to day. Previous research on grading and evaluation of common white Agaricus bisporus mushrooms has revealed that the disagreement between inspectors varied from 14% to 36% (Heinemann et al., 1994). This indicates that standardisation and quantifying the evaluation process by means of machine-based inspection system would benefit starfruit industry and help promote grading consistency. While instruments have previously been developed to inspect agricultural produce, however, most of them do not perform with adequate accuracy when inspection was done on products with non-uniform colour and shape (Abdullah, Aziz, & Mohamed, 2000; Aleixos, Blasco, Navarron, & Molto, 2002; Shearer & Payne, 1990). Consequently, there remains a need for a machine that has the resolution and computational power to inspect starfruits based on colour and shape measurements.

The objective of the work reported in this paper was, therefore, to develop an algorithm and machine vision inspection for automatic grading of starfruits by colour and shape grading. Both the statistical learning and artificial neural network were investigated and results presented and discussed.

2. Methodology

2.1. Grading standard

The Malaysia Federal Agriculture and Marketing Authority (1989) established three grades for golden yellow starfruit belonging to *Averrhoa carambola* L. genus which is used in this study. FAMA grading standards are summarised in Table 1. The grades are FAMA no. 1, FAMA no. 2 and FAMA no. 3 are determined by qualitative and quantitative criteria. The starfruit should be around 635–15 cm long and approximately 9 cm wide. It should has 4–6 pointed star that run from top to bottom. The colour should be translucent green or orange-yellow with minimum darkening or other discoloration. The top grade starfruits are allowed little variation in these quality characteristics, while the lower grade are allowed greater variation and degradation. Generally, starfruits of the same variety do not show significant variation in sizes and weights. The genus investigated in this study belongs to B2 clone. The average weight of B2 clone is approximately 175 g and this weight remains relatively constant for matured fruits (Rahman & Johari, 1992). Therefore, only colour and shape attributes are considered in the present study.

Table 1
Malaysia Federal Agriculture Marketing Authority established three grading standards of ordinary starfruits based on quantitative and qualitative evaluation

Grade	Quantitative/qualitative features	Tolerances (%)
FAMA no. 1	Uniform in colour	5
	Freshness (flesh firmness or texture)	5
	Damage due to mechanical injuries, bruises, diseases, damage by insects affecting more than 25% of fruit surface	5
	Defect (abnormal shape including discoloration affecting 10–25% of fruit surface	5
	Uniform in size (weight > 200 g)	5
FAMA no. 2	Uniform in colour	5
	Freshness (flesh firmness or texture)	5
	Damage due to mechanical injuries, bruises, diseases, damage by insects affecting more than 25% of fruit surface	5
	Defect (abnormal shape including discoloration affecting 10–25% of fruit surface	5
	Uniform in size (weight 120–200 g)	5
FAMA no. 3	Fruit which does not belong to FAMA no. 1 and FAMA no. 2	–

However, establishing discrimination boundaries using colour and shape information usually require inspection and grading by experience human expert. Presently, there are difficulties in enforcing these standards, especially where it entails a large amount of starfruits to be evaluated, made no easier by increasing difficulty in hiring personnel who are adequately trained and willing to undertake the tedious task of inspection. For this reason, this work attempted to standardise the grading scheme of strafruit, thus promoting the quality awareness amongst the planters and producers via machine vision technology. Following FAMA standards, the fruit's colour was used to estimate the degree of ripeness while the fruit's shape was used to determine the overall quality feature.

2.2. Starfruit colour

As mentioned previously, the most reliable method to predict starfruit harvest maturity, and hence marketplace acceptability, is to observe colour and size development. The reasons for colour changes in starfruits are well-understood (Nakasone & Paull, 1998). Similar to other fruits showing a monocarpic behaviour, starfruit appears green at the early of maturity. This colour gradually changes to medium-green when ripe, and ultimately becoming orange yellow when overripe. At the full-colour stage, the fruit ribs are more fragile and easily damaged; hence fruits are normally harvested at the colour break to 50% development, when they have a longer storage life. As skin colour develops, the sugar content increases while the acidity decreases. In other words, mature starfruits have relatively high content of ascorbic acid and very little oxalic acid. In principal, the loss of green colour is due to degradation of chlorophyll contained in special subcellular organelles called chloroplasts. Other colours are due to the range of compounds, including anthocyanins, carotenoids and flavones. In general, degreening is also closely associated with the ageing and decreasing freshness of starfruits after harvest. In this regard, FAMA Standards for grades of starfruits defines three classes of maturity: unripe, underripe, ripe and overripe. Fig. 1 shows group of starfruit image serving as reference for four classes of maturity. Referring to this figure the unripe class exhibits colour of 100% green. This skin changes from green to full yellow as the starfruit matures. The other classes are determined by the green-to-yellow ratio. Hence, the starfruit belongs to the underripe category when less than 25% trace of yellow is present in the skin colour. Meanwhile, the ripe category is when there is 25–75% trace of yellow in the skin colour. Ripe starfruits generally produce soft texture with crisp yellow juicy flesh. Therefore, ripe starfruits are very desirable because they produce best quality products.

Referring again to Fig. 1, it can be seen that the colour of ordinary or nigresens starfruit is highly non-uniform, changing considerably as one moves from the apex to the base of the fruit. The colour appears darker at the apex and at the base, tending to lighter at the centre. Appearance wise the fruit varies appreciably at maturity to light yellowish orange though the apex of the external fruit remains relatively constant. The fruit colour tending to be lighter when ripe, rarely extending over half of the fruit. This colour appears relatively uniform though it may show a lighter or brownish tinge at the edges, covering less than 5% of fruit's surface. Clearly the colour of the ordinary or nigrescens starfruit is generally not constant. This causes difficulty in machine vision inspection since maturity judgement must be based on the colour of the entire fruit. Also, it is equally difficult to allot starfruits with 100% certainty to one of these subgroups as fruits of intermediate appearance can invariably be found. The challenge is, therefore, to develop the pattern recognition software which accurately map the colour changes of starfruits during ripening and use this information as a basis of classification. To classify objects of relatively uniform colour is fairly straightforward since a number of traditional methods such as the table look-up, the threshold-

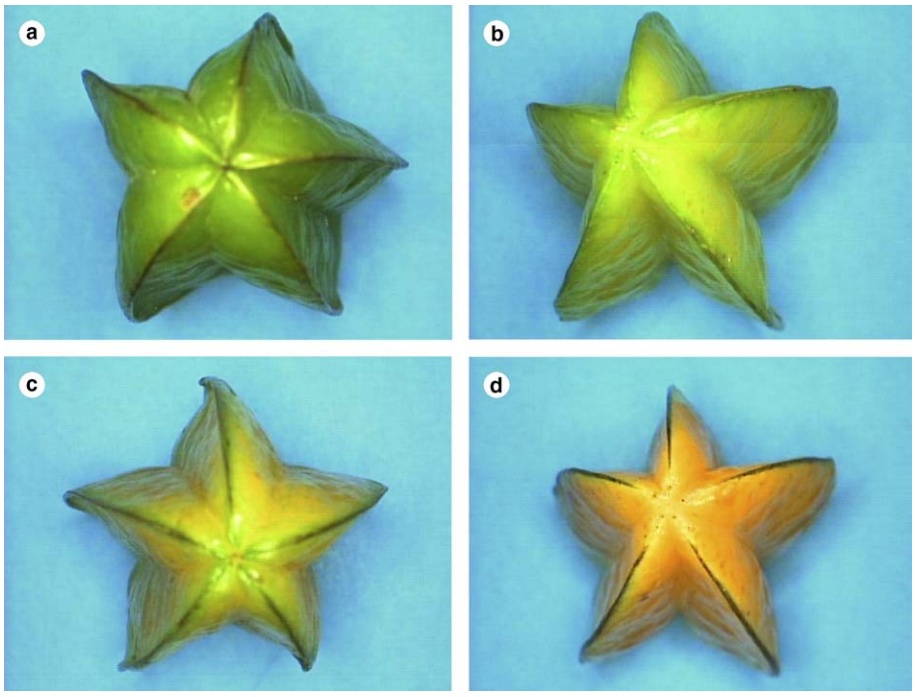

Fig. 1. Group of four starfruit images serving as reference of four different classes of ripeness, (a) unripe, (b) underripe, (c) ripe and (d) overripe.

ing and the nearest neighbour classification work very well. The underlying assumptions may be violated if these methods are applied for classifying images that exhibit a non-uniform colour, causing them to fail (McConnel & Blau, 1995). Hence, a different strategy is needed to solve this problem.

2.3. Starfruit shape

As previously stated, in addition to colour, shape is equally important for quality assessment of starfruits as fruit's shape indicates visually how maturity is progressing. Starfruits have many possible shapes. Their shapes are influenced by the growing environments, resulting various boundary irregularities. Damage during harvesting and handling adds more kinds of shapes. The ideal starfruits, when viewed from the top would take the shape of a star comprising of five strongly pointed longitudinal ridges. Abnormal or misshapen starfruits are those that have more or less than five pointed ridges. Other fruits that exhibit various forms of blemishes also belong to this category. Practically, there is an infinite number of shapes from well to badly shaped starfruits. Unlike parts inspection in manufacturing industry, the shape classification of agricultural produce in not well defined nor uniform. Hence, it is possible for a starfruit to have a shape which the vision system may never have been previously encountered. Prominently, the number of pointed ridges constitutes one of the important attributes which externally characterises starfruits. Hence this attribute was employed by FAMA when developing standards for starfruit grading. The grades are slightly deformed, well formed and seriously deformed corresponding to 4-angled, 5-angled and 6-angled starfruits respectively. Fig. 2 compares the well formed and misshapen starfruits.

The first task in quantifying shape in starfruits was to obtain a profile which would help in shape discrimination. One important and essential criterion for the shape representation is that it must be invariant to translation, scaling and rotation of images of objects. The second task, therefore, was to develop the shape classification algorithm which is insensitive to geometrical transformations and robust with respect to different perturbation such as lighting variations, generalisation outside range of training poses, image noise and object defects. The methods and procedures needed to achieve these objectives are described in the following sections.

2.4. Elements of machine vision inspector

The hardware for typical construction of the machine vision inspection system is relatively standard. All essential elements are shown in Fig. 3. Referring to this figure, the system comprises of the following components: (i) personal computer (PC); (ii) camera, (iii) electronic frame grabber; (iv) illumination device; (v) cables and, (vi) test station. In this work, the frame grabber is the NI-1411 manufactured by National Instrument, USA. This device is equipped with 8-bit A/D converter having optical resolution of 640×480 elements. It was mounted into the vacant PCI slot Pentium III PC

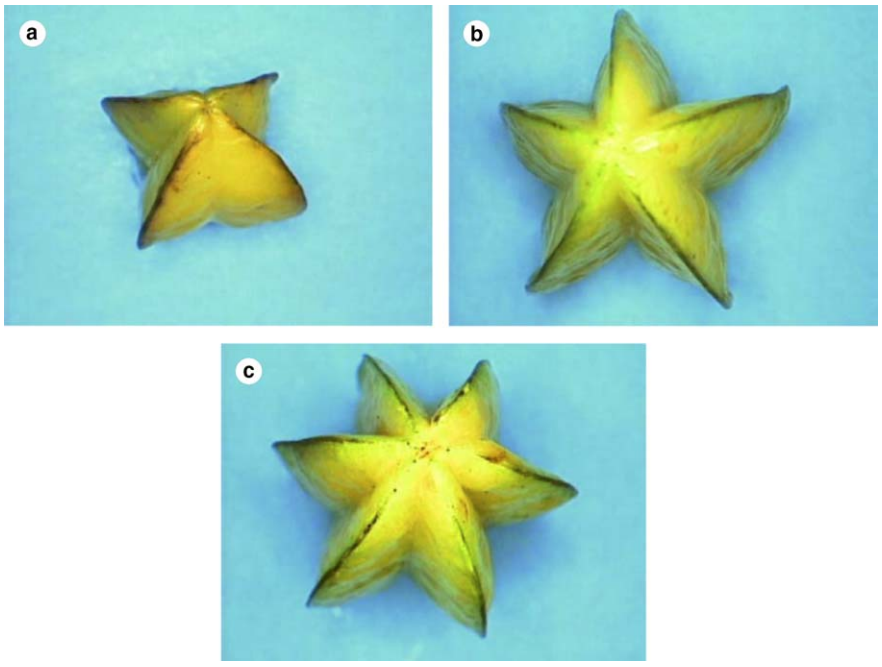

Fig. 2. Top view examples of (a) 4-angled, (b) 5-angled, and (c) 6-angled starfruits corresponding to slightly deformed, well formed and seriously deformed grades respectively.

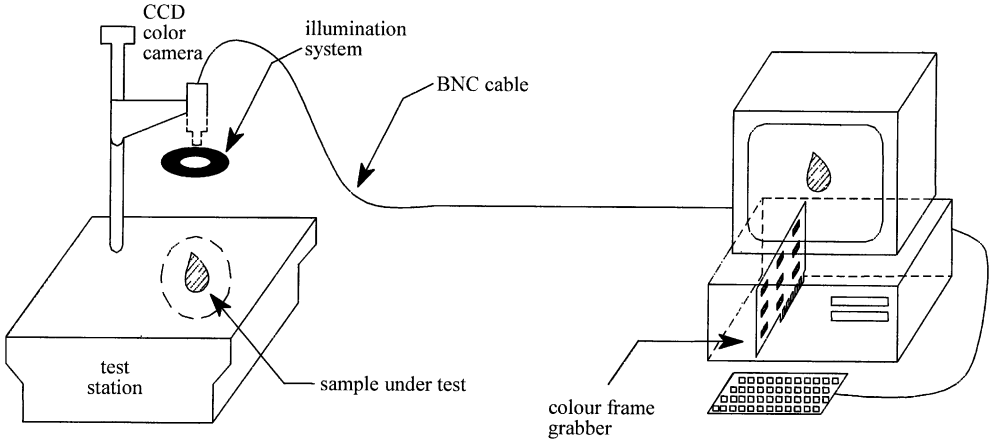

Fig. 3. Elements of machine vision inspection system.

running at a clock speed of 450 MHz with 64 MByte of RAM size. These configurations enabled images be digitised and displayed at a sustainable rate of 30 full frame per second. This speed was more than adequate for starfruit imaging application described in this paper. The camera was the CS5260D CCD type colour camera manufactured by Tokyo Electronics Industry, Japan. It comes with standard C-mount type optical lens and connected to frame grabber via 2 m external BNC cable. The camera was mounted to a $13'' \times 18'' \times 0.5''$ anodised aluminium platform via 90° angle mount horizontal arm, forming the test station of machine vision system. The later was illuminated using warm white deluxe (WWX) ultra high-frequency fluorescent light ring. The WWX bulb had a colour rendering index of 79 and colour temperature of 6000 °K. The bulb was fitted with continuous light intensity control which allowed 10–100% intensity adjustment and almost 360° diffuse illumination which are important for successful application of machine vision system.

The software for machine vision inspector comprised of three principal layers: low-level processing, intermediate processing and high level processing. In summary, the first layer involved image acquisition and pre-processing such as image enhancement, extraction and restoration. Meanwhile, the second layer concerned with image transformation, segmentation and filtering. Finally, the third layer involved image recognition and inter-

pretation. All image subroutines in these different layers were coded using National Instrument NI-IMAQ vision module running on Labview 6.0 programming environment. In this case, the NI-IMAQ was quite useful since it has a special routine which converts NTSC composite S-video signal to Hue, Saturation and Intensity (*HSI*) work space in almost real-time.

3. Artificial inspector

3.1. Colour inspector

The objective of colour inspector is to allocate the starfruit of unknown origin to the appropriate group, corresponding to unique maturity or ripeness index based on colour measurement. Fig. 4 shows hue distributions of starfruits by four grade categories. In this space, only the H component was plotted since this variable concurs almost exactly with the accepted physiological model of colour vision (Celenk, 1990). The graph in Fig. 4 clearly demonstrated that the starfruits are not uniform based strictly on quantitative hue values, but rather show colours that tend towards yellowish orange (21–22) and translucent green (48–51) for overripe and unripe cases respectively. The starfruit's colour angularly shifted in anticlockwise direction towards low hue values as maturity is progressing. Further inspection of Fig. 4 revealed that there is a slight decrease in hue value at the early stage of maturity. In contrast, the hue value increases drastically as starfruit enters senescence stage. As a result, both the overripe and ripe classes could easily be distinguished, whereas, the unripe and underripe classes are less easily distinguishable. Also, it can be seen from Fig. 4 that the hue distributions of each class of starfruit are not uniform but overlap each other. Consequently, the number of pixel counts near the cut-off thresholds is significantly large, an increase or decrease in the threshold of one class will result in a good number of starfruits being misclassified. Clearly, no single threshold exists that can uniquely separate one class of starfruits from another. Moreover, the presence of image noise can easily affect these distributions as some unwanted noise may appear in the same range in starfruit hue. Therefore, the challenge is to device an artificially robust strategy which can uniquely discriminate and classify starfruits into groups or clusters based on a hue measure or ripeness spectra. Presently, there are various techniques which can be used to solve this type of pattern recognition problem. Du and Sun (2004) reviewed recent advances in artificial intelligent techniques used in solving food engineering problems. Among the methods which have found successful applications in food industry, the discriminant analysis and the neural network appeared two most widely used techniques. Hence, these methods were also investigated for ripeness detection and classification of starfruits. Brief description of these techniques are given in Sections 3.1.1 and 3.1.2 respectively.

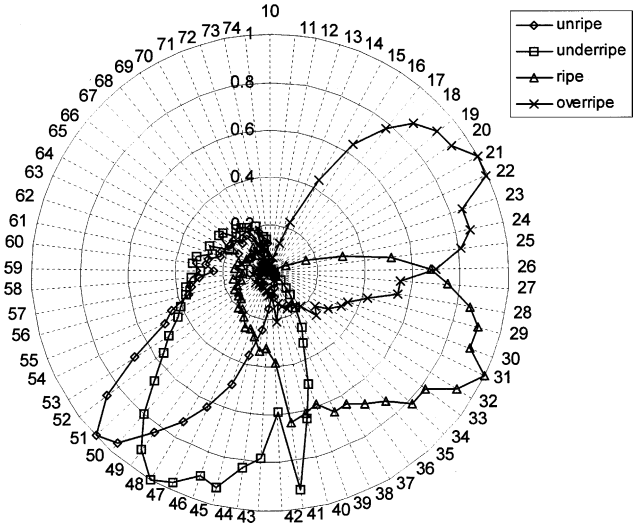

Fig. 4. Ripeness chart showing hue distributions of starfruits by four grade categories. Over 10 samples were averaged for each grade.

3.1.1. Discriminant analysis (DA)

In the strictest sense, DA is the study of system of random variable or random samples emanating from different groups, and the problem is allocating an object of unknown origin to appropriate group. Hence, DA is well suited for studying the relationship between colour and grade during machine vision inspection of starfruits. Furthermore, this technique is relatively easy to implement, fast and fairly accurate. Abdullah, Guan, and Mohd-Azemi (2001) have published detailed mathematical explanation, strategies and techniques involved in applying DA for machine vision applications. The discussion here, therefore, will be restricted to important practical aspects of the technique applied for developing colour-maturity discriminant models of starfruits, without getting into details of complete computational formulae.

Assuming that the hue distributions from g group population are characterised by multivariate normal distributions having averaged hue vector $\overline{h_i}$ and the within-group covariance matrix Σ_i for $i = 1, 2, 3, \ldots, g$, then the probability density function for the ith group is given by:

$$f_i(h) = \frac{1}{|\Sigma_i|\sqrt{(2\pi)^p}} \exp\left[-\frac{1}{2}D_i^2\right] \tag{1}$$

where p is the total number of hue variable; D_i^2 is the popular Mahalanobis' distance defined as:

$$D_i^2 = (h - \overline{h_i})^{\mathrm{T}} \Sigma_i (h - \overline{h_i}) \tag{2}$$

In Eq. (2), h represents the p-dimensional hue vector and "T" indicates the matrix transpose. Defining the likelihood of each group statistically as:

$$U_i = \log f_i(h) \tag{3}$$

therefore, the logarithm of $f_i(h)$ in Eq. (1) can be written as:

$$U_i = -\frac{1}{2}\{(\log|\Sigma_i| + p\log(2\pi)) + D_i^2\} \tag{4}$$

Similarly for jth group

$$U_j = -\frac{1}{2}\{(\log|\Sigma_j| + p\log(2\pi)) + D_j^2\} \tag{5}$$

We discovered Eqs. (4) and (5) were experimentally difficult to manipulate because of two major problems. Firstly, there was unlimited number of h values in HSI space that could be used to produce U_i or U_j. However, not all of them are necessarily independent or uncorrelated variables. In fact some of them are redundant and they do not have sufficient discriminating power. Therefore, these variables need to be eliminated. Statistically, such an elimination will not only reduce the dimensionality or the interdependence of variables among themselves, but, more importantly, it improves the correct-to-false classification ratio (Gombar & Enslein, 1991; Smith & Nakai, 1990). Consequently, selecting a best subset of h values before performing discrimination is generally an attractive classification strategy. We implemented this strategy by invoking the Wilks-Lambda analysis (Rencher & Larson, 1980). The second problem was concerned with the covariance matrices which were not equal or heteroscedastic. The problem was primarily due to the environmental effects, particularly the instability of lighting intensity levels which occurred inherently. We observed that the machine vision system was quite sensitive to the instability of the illumination system, changing as much as 13–42% for a small change in the lighting intensity levels. This finding is consistent with findings on lighting used in image processing for greening detection of potatoes (Heinemann, Varghese, Morrow, Sommer, & Crasweller, 1995). We solved this problem by firstly approximating the within-group covariance matrix with the average pooled-covariance matrix. Mathematically,

$$\widehat{\Sigma} = \frac{1}{g}\sum_{i=1}^{g}\Sigma_i \tag{6}$$

Secondly, substituting Eq. (6) into Eq. (4) and after linearising yields

$$\widehat{U}_i = -\frac{1}{2}\{\log|\widehat{\Sigma}| - \log K_i - D_i^2\} \tag{7}$$

where $\widehat{U}_i$ is the ith linear discrimination function, and, K_i is the ith classification function. Using Eq. (7) we discriminated starfruits into group having the highest $\widehat{U}_i$ (Morrison, 1967).

3.1.2. Neural networks (NN)

Neural networks have been successfully employed in numerous applications, ranging from data forecasting to medical diagnostic. Unlike DA, the NN based learning is more appropriate in many non-parametric tasks when variables are highly independent and no known mathematical model is yet established. Generally, NN are constructed of many processing elements (PEs) that are linked in a certain way. Fig. 5 shows a general structure of the multi-layer preceptron (MLP) neural network which is investigated for application described in this paper. The detailed description on MLP is given elsewhere (Haykin, 1999). Essentially, the MLP comprises of three different layers: input layer, hidden layer and output layer. The hidden layer maps the input pattern h with output pattern y through a series of interconnected weights. Mathematically,

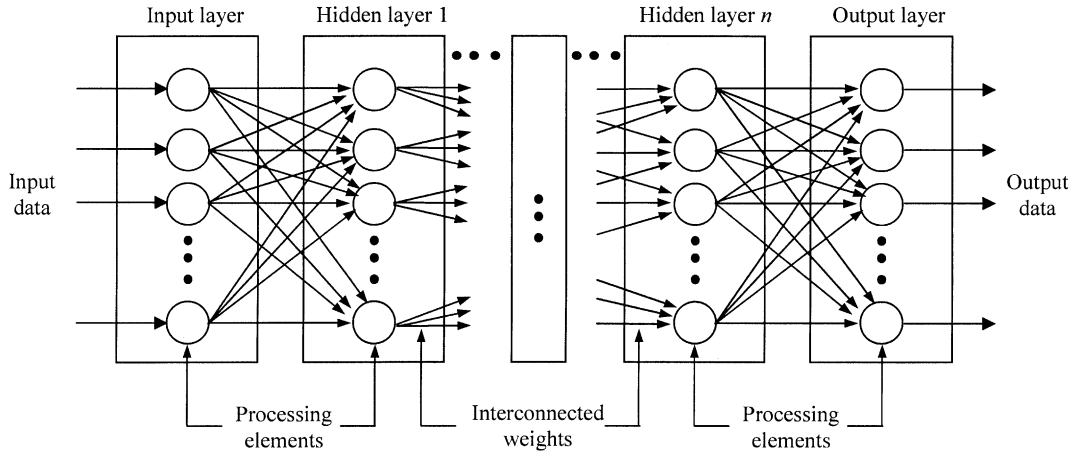

Fig. 5. Multi-layer perceptron neural network with an input layer, n hidden layers and an output layer.

$$S_j = \sum_{i=1}^{n} W_{ij} h_i \tag{8}$$

where S_j is the output from jth PE; W_{ij} is the weight of the ith input vector which is connected to jth PE. Following this equation, learning in NN implies that the PE change the output in response to the input change by adjusting the connecting weights. In so doing, S_j must be further processed by the activation function, resulting in the final neuron's output signal such as:

$$y_j = f(S_j) \tag{9}$$

The activation function determines the processing inside the neuron. It can be linear or non-linear function depending on the network topology. In this work, the logarithmic and hyperbolic type tangent functions were selected. Respectively, these functions are given by,

$$f(s) = \frac{1}{1 - e^{-s}} \tag{10}$$

and,

$$f(s) = \frac{e^{s} - e^{-s}}{e^{s} + e^{-s}} \tag{11}$$

Two important factors must be considered in order to ensure a successful application of MLP based NN. First is the number of hidden layers and second is the number of PE. In general the MLP with too few hidden layers will not have a sufficient capability to accurately represent the input–output relationship. In contrast the MLP with too many hidden layers may lead to a problem of data overfitting, affecting the system's generalisation capability. Hence, determining the optimal number of hidden layers is a very crucial step in designing the MLP classifier. However, such a determination is not an easy task since it depends largely on a designer's experience and trial-an-error method. Our design approach was to firstly start with one hidden layer having only input and output PEs, and secondly, systematically growed the network by adding one hidden layer at the time. In order to do this, the network growing technique such as the cascade-correlation method was implemented (Fahlman & Lebiere, 1990). In contrast, fixing the number of output PEs is a very straightforward procedure. This number corresponds to the number of categories needed to represent the input pattern. In this case, four binary outputs were used corresponding to four grading categories of starfruits.

Once the number of hidden layers have been established, the network was trained using data from training set. In this way the MLP was able to learn the complex and non-linear relationship between colour and maturity of starfruits. In this case, the network was trained using the modified back propagation algorithm together with the Bayesian regularisation technique (MacKay, 1992). In summary these methods work by minimising the sum squared error between the actual and MLP estimated data. Theoretically, a trained network can be used for other similar data sets.

3.2. Shape inspector

Presently there are various techniques for shape detection and shape separation that have been investigated and experimented. In summary, these techniques can be summarised into four basic categories: (i) encoding such as centroid contour distance, chain codes and media axis transform (ii) statistics such as moments, bending energy, radius variation and fractals (iii) morphological structure such as skeletonisation and thinning, and (iv) spectrum. Although many general techniques were documented in computer vision literature, the natural variability and diversity of biological materials create difficult and practical problems. These techniques can be used effectively for solving well-defined shape problems or shapes that can accurately represented by unique mathematical models. Based on studies and various experiments, it was proven that most of these techniques were not adequate nor had enough power for shape discrimination of starfruits because different shapes may have the same value. In contrast, the method conceptionalised by Zahn and Rookies (1972) that used the Fourier descriptors seems to be more attractive. The main reason for this is that this method uses global image descriptors instead of the local ones. This method is more applicable to real-world images in which simple and multiple point features may be difficult to extract, and eliminating the need for feature matching between reference and observed images. Another unique feature which makes Fourier descriptors a clear advantage over other techniques is that the representation is invariant to translation, rotation and scale changes. Therefore, much research has also been conducted further on the basic algorithm to achieve better performance and efficiency. There also have been some successful applications reported in the literature (Heinemann, Pathare, & Morrow, 1996; Paliwal, Shashidhar, & Jayas, 1999). Therefore the Fourier descriptors have been investigated for use in shape discrimination of starfruits.

The first task in quantifying shape using Fourier descriptors was to obtain a profile, depicting the boundary of the object's image. The next step was to extract the image features that geometrically describe the pose of an arbitrary object. In so doing, the points corresponding to object centroids were computed from first-order geometric moments. The relationship between moments of an arbitrarily shape object with known boundary co-ordinates and centroid is given by Green's theorem (Tao, Morrow, Heinemann, & Sommer, 1995). Mathematically,

$$x_c = \frac{\sum_{k=0}^{N} y_k (x_k^2 - x_{k-1}^2) - x_k^2 (y_k - y_{k-1})}{2\sum_{k=0}^{N} y_k (x_k - x_{k-1}) - x_k (y_k - y_{k-1})} \tag{12}$$

and,

$$y_c = \frac{\sum_{k=0}^{N} y_k^2 (x_k - x_{k-1}) - x_k (y_k^2 - y_{k-1}^2)}{2\sum_{k=0}^{N} y_k (x_k - x_{k-1}) - x_k (y_k - y_{k-1})} \quad (13)$$

where (x_c, y_c) is the centroid; (x_k, y_k) is the co-ordinate of kth boundary pixel; N is the total number of boundary pixel defined in a clockwise direction from a fixed starting point. Using Eqs. (12) and (13), the distance of each boundary pixel to the centroid can then be calculated as follows:

$$R(k) = \sqrt{(x_k - x_c)^2 + (y_k - y_c)^2} \quad (14)$$

The Fourier transform of $R(k)$ yields a one-dimensional feature vector, corresponding to the desired Fourier descriptors of the object. Such a transformation is given by:

$$F(m) = \frac{1}{N} \sum_{k=0}^{N} R(k) \left[\cos\left(\frac{2\pi mk}{N}\right) - j \sin\left(\frac{2\pi mk}{N}\right) \right] \quad (15)$$

where m is the order of $F(m)$. Alternatively, the magnitude of $F(m)$ can be calculated as follows:

$$|F(m)| = \frac{1}{N} \times \sqrt{\left[\sum_{k=0}^{N} R(k) \cos\left(\frac{2\pi mk}{N}\right)\right]^2 + \left[\sum_{k=0}^{N} R(k) \sin\left(\frac{2\pi mk}{N}\right)\right]^2} \quad (16)$$

Eq. (16) produces a pattern or signature which uniquely describe the shape of the object. In theory, the order of Fourier descriptors ranges from zero to infinity. However, one favourable property common to Fourier descriptors is that the high quality boundary shape representation can be obtained using only few lower-order coefficients. Therefore, only the first six coefficients were selected in this research for shape recognition. Generally, translation, scaling and rotation invariance is expected as the pattern generated by Fourier descriptors is relative to the object centroid, and hence, it is invariant to object scaling. A robust scaling normalisation and an effective and efficient starting point location method was introduced to achieve invariance.

4. Materials and methods

4.1. Sample preparation

Industrial grade starfruits belonging to *Averrhoa carambola* L. genus were sourced from local farms and packing houses. Here, the quality grades of each fruit were inspected, packed and transported to laboratory within 24 h to avoid degradation of colour and induced maturity. All fruits were again re-inspected in the laboratory using semi-trained panel. The panel comprised of several college-age students since FAMA trained inspectors were not easily available. The inspectors studied the starfruit one at a time and made judgement as to a fruit quality. Damaged fruits and fruits infected by insects, diseases, birds including various form of mechanical injuries were discarded. Depending on the quality feature, the inspection time ranged from less than a seconds to tens of seconds. Nearly 300 samples of starfruits were inspected and categorised either as training or test samples. The first 80 test samples, comprising of 20 samples for each grade formed the training set. The remaining samples, comprising of 50 samples for each grade formed the test or independent set. All samples in the training set were used to train and subsequently evaluate the consistency of machine vision system. Meanwhile, the test samples were used to evaluate the accuracy of trained machine vision system. In so doing, all starfruit samples were imaged and the captured data were digitised and sent to PC for inspection.

4.2. Colour analysis

In assessing the starfruit maturity based on colour vision inspection, the machine inspector, namely the CCD

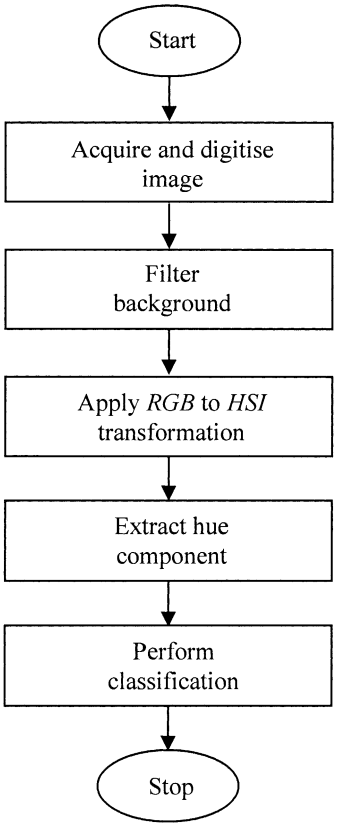

Fig. 6. The overall procedure for starfruit maturity classification based on colour perception.

camera must be calibrated so that its response would be most sensitive to light wavelengths reflected from the feature of interest. Most importantly, the background should be of a shade that reflects light in a range which falls outside to those reflected by starfruits. Since starfruit hue ranges from 10 to 74 for all quality grades, therefore, any hue colour which falls outside this range is suitable candidate for background shade. In this work the cyan corresponding to digital hue of 127 was used as background colour. This has resulted in good contrast image which is important for accurate image representation. Calibration was performed by exposing the camera to this background shade and, adjusting the illumination intensity and brightness level until the error between measured and calculated hue value converged to less than 1%. Inspection was carried out by capturing a single starfruit image and transforming and compressing the RGB data to hue values. The resulting image was fed to either DA and MLP for establishing fruit maturity or grade. The flow chart in Fig. 6 summarises the overall procedure for colour classification.

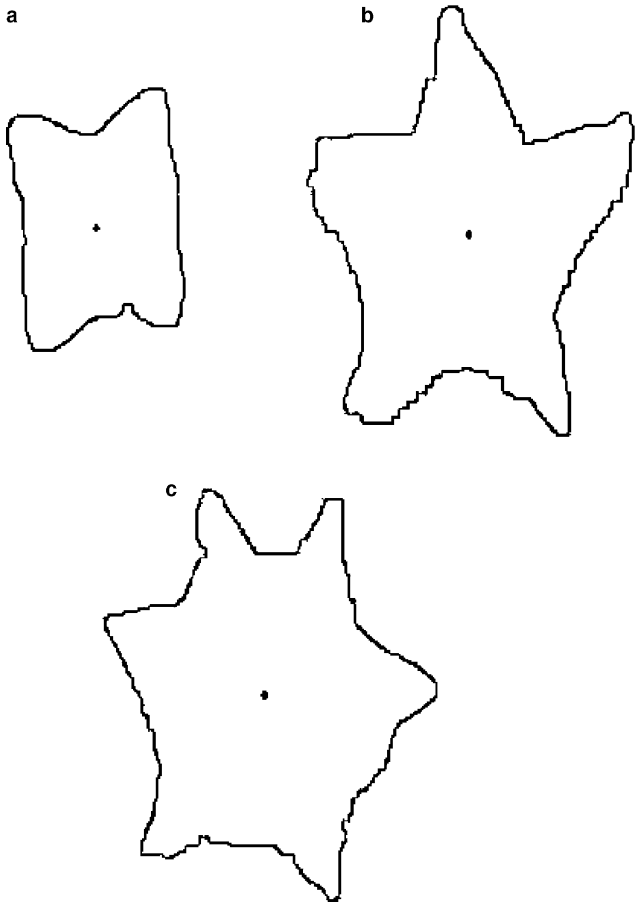

Fig. 7. One dimensional boundary patterns corresponding to starfruit shapes in Fig. 2. The solid dot shows the centroid for each shape calculated using first-order geometric moments.

4.3. Shape analysis

As stated previously in Section 3.2, the objective of shape analysis is principally to extract the Fourier descriptors by using Eq. (6). Hence, some form of image processing is needed in order for the machine vision to

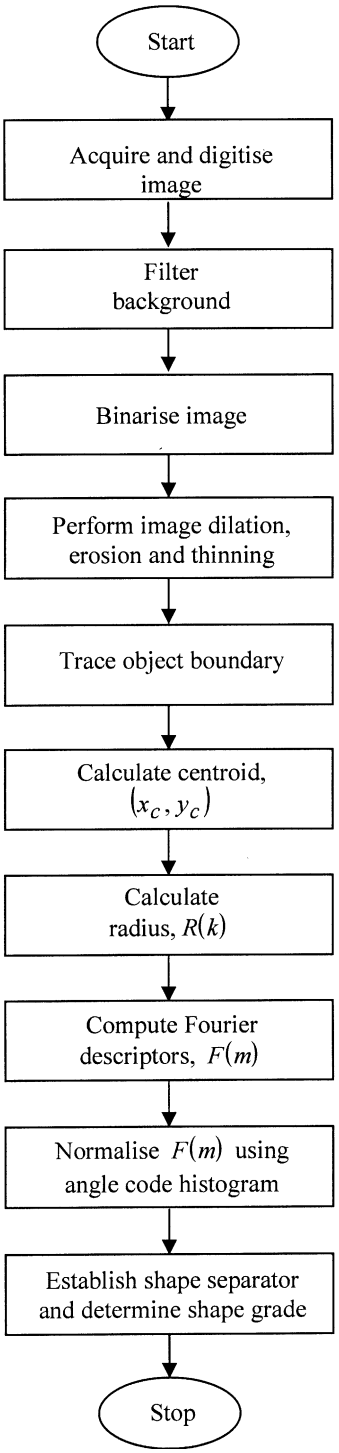

Fig. 8. The overall procedure for starfruit shape classification.

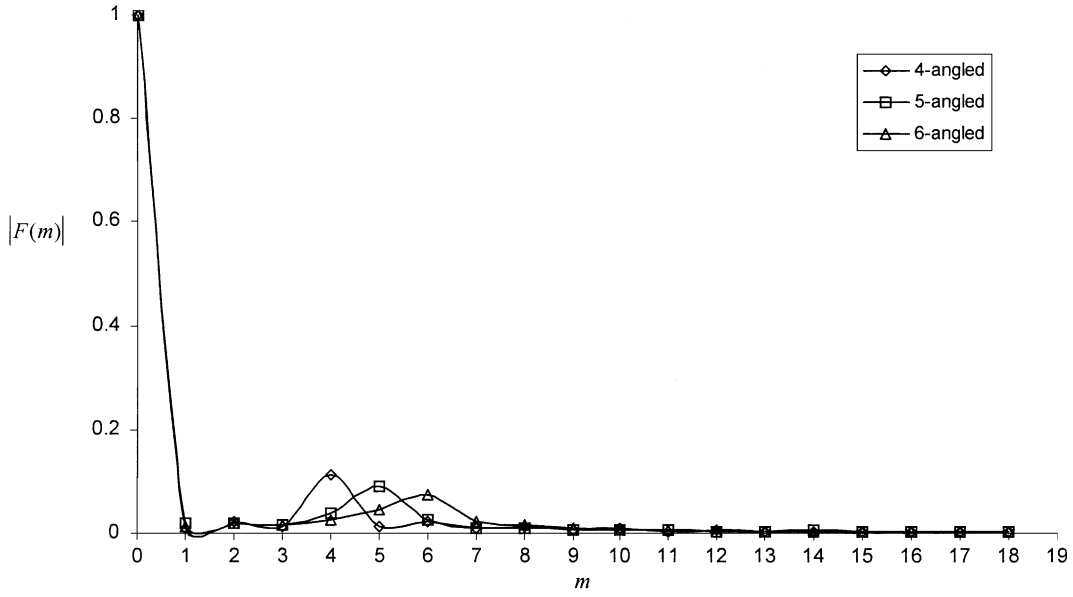

Fig. 9. The plot showing the distribution of normalised Fourier descriptors for each starfruit shape. Both the dc value and harmonics are plotted.

quantitatively analyse image feature and produced data needed for further analysis. The first step was to filter the unwanted information such as background pixels and spots due to presence of highlights and shadows. Since the machine vision produced high contrast image, it was possible, in this case, to accurately segment all pixels belonging to starfruit's hue using direct thresholding. The cut-off value was adaptively and globally decided based on image scene. The next step was to extract image components that are useful in the representation and description of region and shape, such as boundaries and skeletons. In so doing, the image was processed using series of morphological operations such as dilation, erosion and thinning. Among these techniques, thinning is perhaps the most important operation since it eliminates redundant information but retains the topological information concerning the shape and structure of the object. A number of algorithm are available to implement this operation. In the present case, a non-iterative approach employing line-following or length-encoding method was employed since this technique emulates the way human being would perform thinning (Baruch & Luew, 1988). Fig. 7 illustrates the boundary images of starfruits generated using the above morphological operations. The resulting image was used to calculate the moments and finally the Fourier descriptors of the object. As earlier stated, changing the object size will affect the number of boundary points and hence, altering the amplitude of Fourier descriptors. To enable recognition between Fourier descriptors possible, these changes should be accommodated by normalisation. A straightforward normalisation would, however, result in a partial of full loss of contour details such as ripples or isolated discontinuities. An angle code histogram was adopted to compensate for this problem (Peng & Chen, 1997). Fig. 8 summarises the overall procedure taken for shape analysis, and, a graph in Fig. 9 shows the plot of normalised Fourier descriptors for each shape category. Clearly from Fig. 9, the 4-angled, 5-angled and 6-angled starfruits can uniquely be characterised by $|F(4)|$, $|F(5)|$ and $|F(6)|$ respectively, suggesting that shape separation could be established using direct thresholding method.

5. Results and discussion

5.1. DA learning

The objective of DA learning is principally to identify a subset of dominant features that are most responsible for splitting a set of observations into two or more groups. Frequently, the successful application of colour recognition using machine vision system relies strongly upon the choice of proper spectral range and the number of variables employed in the calibration model. In this study, we have conducted the step-wise discriminant analysis by invoking the Wilks-lambda analysis to select the best subset containing principal hue values. In so doing the system was trained using training data comprising of 20 samples for each group. The hue range from 10 to 74 formed the initial input data set. The Wilks-lambda method analysed these data, detecting both the insignificant and highly insignificant or potent hue variables. This method of variable selection operates in iterative manner, systematically removing hue variables whose F-statistics which are smaller than F-to-remove, and, retaining those values whose F-statistics

are greater than *F*-to-enter values. The *F*-to-remove and *F*-to-enter values chosen for this applications were 2.71 and 2.84 respectively, the common statistical cut-off points in multivariate discriminant analysis (Dillon & Goldstein, 1984). The algorithm converged in five steps, resulting in subset containing 12 principal hues with eigen values greater than 1.0. Thus the dimensionality of the data was reduced from 65 correlated hue values to 12 uncorrelated principal components with a 81.5% loss of variation. The proportion of variance explained by any one of principal component was not greater than 10% and the individual peak loadings on the principal components were relatively uniform. The principal hues selected through this step-wise analysis were 24, 26, 32, 33, 41, 48, 49, 55, 56, 64, 73 and 74. It should be noted that these values were not all in the green range. In fact hue 73 and hue 74 lie in the yellowish region, indicating that some features in the non-green range had significant discrimination power. The discrimination power of these principal hues can be examined by studying the Mahalanobis' distances which are shown canonically in Fig. 10. This plot clearly demonstrates that the starfruits separate into four groups, corresponding to four different grades or maturities. A close inspection of Fig. 10 reveals that overripe and ripe groups separate distinctively among themselves in a similar manner to that of unripe and underripe groups. However, the Mahalanobis' distance between unripe and underripe groups is significantly smaller compared to overripe and ripe groups. This is due to minor colour differences between unripe and underripe groups. Therefore, the potential of misclassification between these two groups are higher compared to other groups. However, it was heuristically discovered that as long as the Mahalanobis distance is at least 10% of the maximum distance in the group, then a unique classification could still be guaranteed.

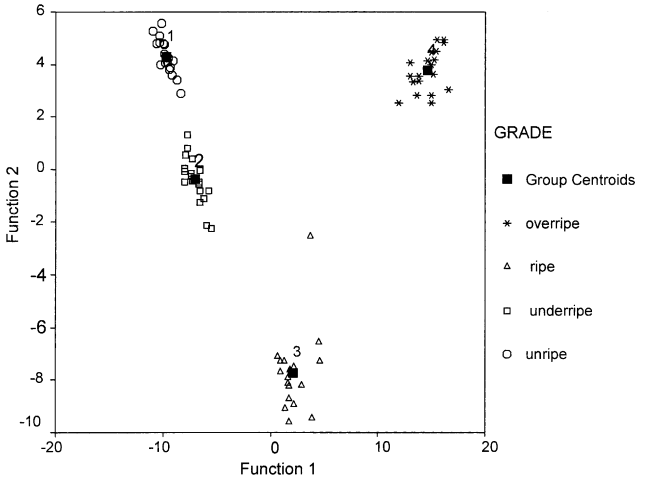

Fig. 10. A canonical plot showing the discriminant separation by starfruit grades. The plot was produced using 12 principle hues and averaged from 20 samples for each grade.

5.2. MLP learning

As stated previously, the objectives of MLP learning are primarily to establish the number of hidden layer and the number of PEs in each hidden layer. Investigation was performed to investigate the relationship between system performance and number of hidden layer. It was noticed that the MLP's performance did

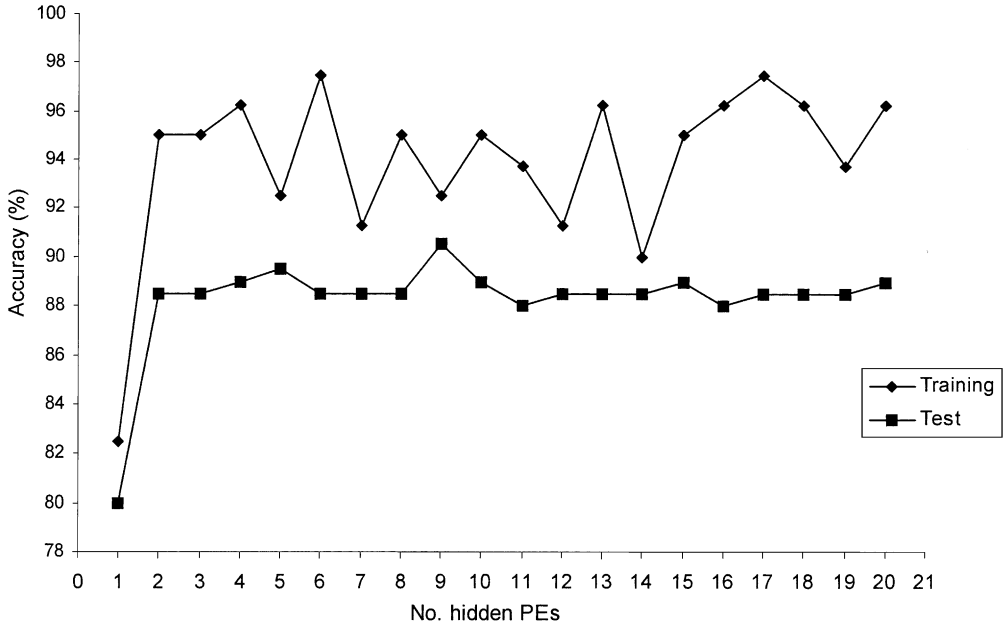

Fig. 11. MLP training and testing accuracies for various numbers of PEs over selected hue features.

not show any significant improvement when the number of hidden layer was increased from one to two or three layers. Consequently, a single hidden layer MLP was designed for this application. The training was, therefore, reduced to determining the number of PEs in the hidden layer. Fig. 11 shows the training and test accuracies for different number of PEs. It can be seen from this figure that the MLP with one hidden PE resulted in the lowest training and test accuracies. Clearly, a single PE could not accurately and efficiently map the relationship between colour and maturity of starfruits. Meanwhile, the highest training accuracy of 97.5% was produced when 6 hidden PEs was employed. However, this MLP was not necessarily the best or optimal system since it yielded a test accuracy of 88.5% only. This problem was caused by data over-fitting in which the MLP seemed to memorise the input patterns belonging to training samples, thus, affecting its capability to generalise. The results in Fig. 11 suggest that overall, the presence of more PEs resulted in increasing accuracy. This trend continued up to 9 hidden PEs after which, the accuracy fluctuated between 88% and 90.5%. Therefore, the 9 hidden PEs corresponding to 92.5% and 90.5% training and test accuracy respectively was employed for MLP grading of starfruits.

5.3. Starfruits colour grading

Both DA and MLP methods were tested using training and test samples. In addition, experiments were also

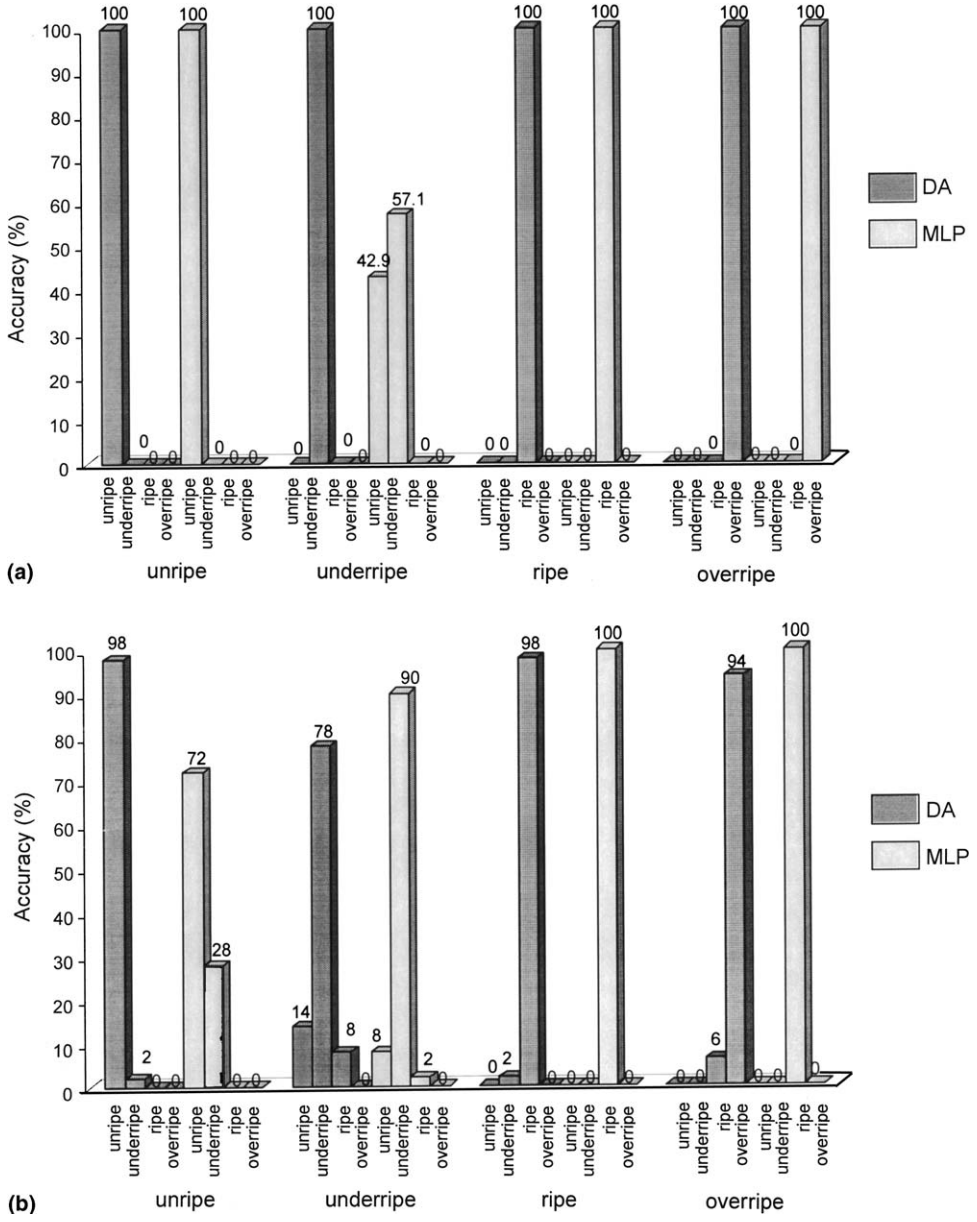

Fig. 12. DA and MLP classification results after Wilks-lambda analysis of (a) training samples, and (b) test samples.

performed using all features from hue 10 to hue 74 in order to establish the relationship between system's performance and dimensionality reduction. Training and test results using selected features resulted from Wilks-lambda analysis are shown in Fig. 12(a) and (b) respectively. In case of training samples, DA produced 100% correct classification compared to 89.3% for MLP. These results suggest that DA is more efficient in learning the relationship between colour and fruit maturity despite limited number of samples. The performance of each classification method can be verified by examining Fig. 12(b) which tabulates results from test samples. Referring to this figure, DA performed on 12 principal hues yielded a percent correct classification of 95.3% compared to 90.5% for MLP by starfruit variety. A difficulty in classifying unripe and underripe is evident from this figure. DA showed a greater than 88% average correct classification for unripe and underripe grades. However, the average correct classification of MLP for these grades was 81% only. These results give some indication on the overall performance of DA and MLP for colour grading of starfruits.

The classification results using all features from hue 10 to hue 74 are shown in Fig. 13(a) and (b). For the training process, the average correct classification rates for DA and MLP were 77.5% and 95.7% respectively. Clearly, the MLP performance has increased slightly when all features were used. In contrast the classification power of DA was higher when using fewer hue values than when using the full range of hue values. This trend

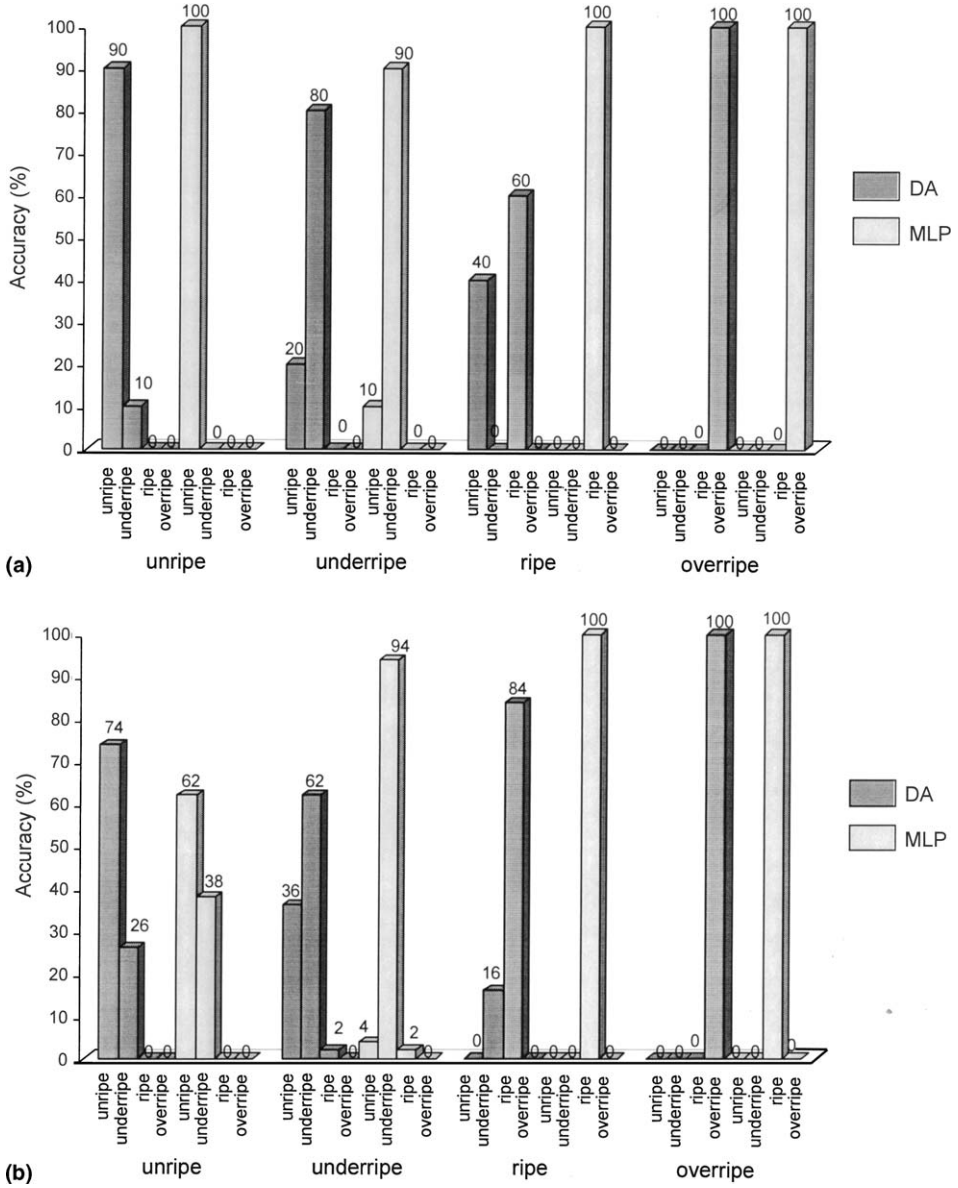

Fig. 13. Classification results from direct applications of DA and MLP of (a) training samples, and (b) test samples.

can be validated using results from test samples shown in Fig. 13(b). The average correct classification rates of DA and MLP were 80% and 89% respectively. Even though DA recorded a slight increase in the classification rate for test samples, however, the overall success rates were consistently lower compared to cases when fewer hues were used. The average correct classification rate for MLP, however, remained relatively unchanged when using full range hues. Therefore, it can be concluded that DA after Wilks-lambda analysis is more precise in classification than direct application of discrimination analysis. These results also suggest that DA had reasonable discrimination power compared to MLP, but less than that when using all features.

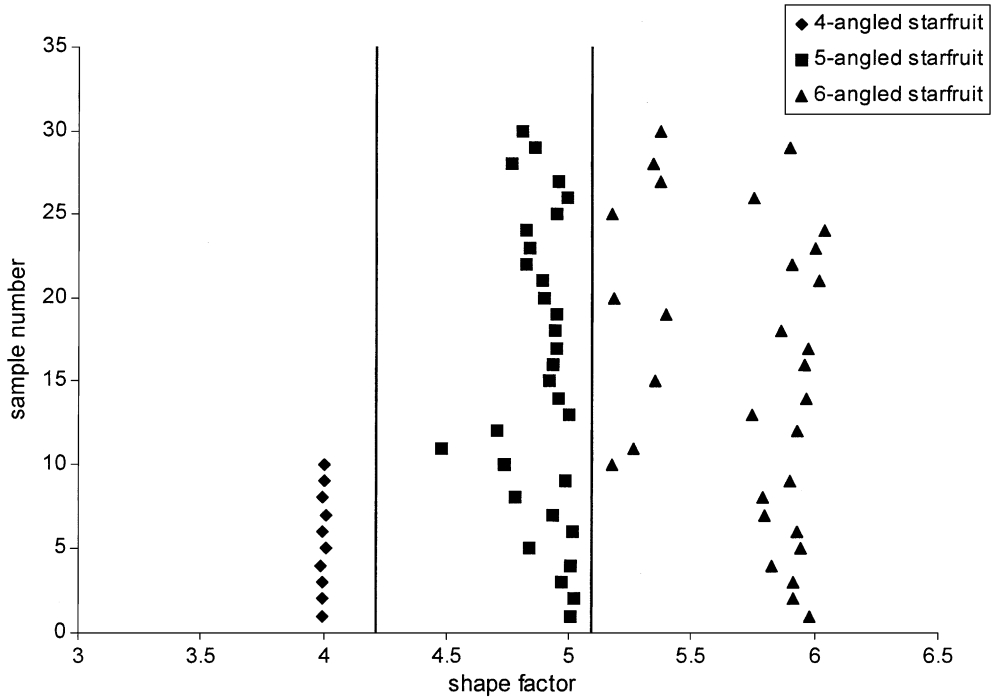

Fig. 14. Distribution of starfruits by the shape factor defined by FAMA's standards. The vertical lines indicate shape factor boundaries.

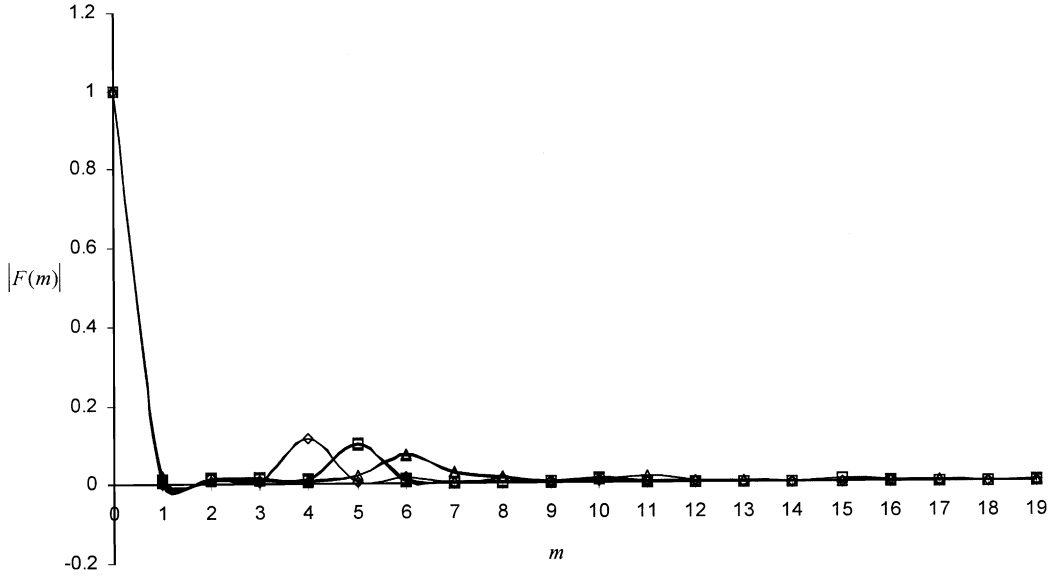

Fig. 15. Comparison of boundary signature patterns for each shape category of starfruit before and after rotations: (◇) 4-angled starfruit, (□) 5-angled starfruit and (Δ) 6-angled starfruit. The overlapped curves are boundaries of the original and, with 90° rotation, 180° rotation and 270° rotation.

5.4. Starfruits shape grading

The method of shape separation was experimented on several batches of samples. Prior to experiments, the sample starfruits were inspected and graded into shape categories using professional inspector. The result of a test on 70 starfruit samples with random shapes is shown in Fig. 14. It can be seen from this figure that the shape factors formed three distinct bands corresponding to three shape categories of starfruits. Hence it was possible to determine the suitable cut-off thresholds for the shape factors. The vertical lines drawn in Fig. 14 indicate shape factor boundaries. Referring to this figure, the shape factors for most of 4-angled starfruit were consistently less than 4.3, the shape factors for 5-angled starfruits lie between 4.3 and 5.1, and the shape factors for 6-angled starfruits were consistently greater than 5.1. Hence, choosing these cut-off thresholds, it was practically possible to achieve 100% correct classification of starfruits by shape categories. It can also be observed in Fig. 14 that there is very clear demarcation between 4-angled and 5-angled or 6-angled starfruits. Therefore the 4-angled starfruits can be easily separated from 5-angled or 6-angled shape category. However, the boundary separating 5-angled and 6-angled starfruits is relatively small, implying, the potential of misclassification between these two shape categories is relatively high. However, an optimum classification can still be guaranteed provided that the threshold value is correctly chosen.

This method of shape analysis was also tested for verifying the independence of rotation and size of starfruits. The original inspection designed allowed a starfruit to be positioned at any location and orientation as long as it was in the image space. This means that applying the method for a starfruit in different orientations and sizes should yield the same result. Two experiments were designed in order to confirm this hypothesis. In the first experiment, the size of starfruit was fixed but the image was captured with four different rotations: 0°, 90°, 180° and 270°. These procedures were repeated for each shape category of starfruits. The normalised shape factors for each image were calculated and shown graphically in Fig. 15. Clearly from this figure the dimensional boundary curves for each shape category showed the same overlap. The cut-off threshold remain relatively unchanged for all cases. Furthermore it was discovered that the standard deviations for harmonic components obtained from discrete Fourier transform were indeed very small. This shows that this method is highly independent of rotation. In the second experiment, the rotation was fixed but the image size was scaled. Respectively, four scaling factors were introduced: −70%, −50%, +50% and +70%. In the same way, the normalised shape factors were calculated for each scaled image and for each shape category. The plots are shown in Fig. 16. The shape factors of the original unscaled image were also included for comparison purpose. Again as illustrated clearly in Fig. 16, the boundary patterns of the scaled and original images

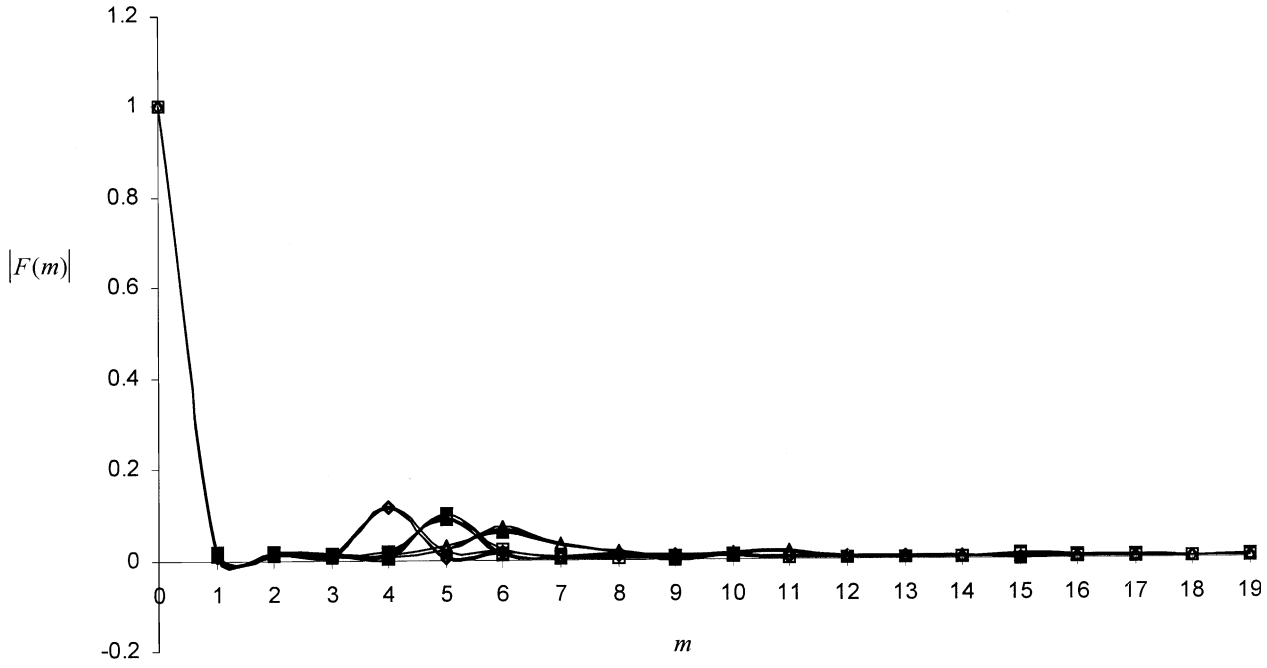

Fig. 16. Comparison of boundary signature patterns for each shape category of starfruit before and after scalings: (◇) 4-angled starfruit, (□) 5-angled starfruit and (Δ) 6-angled starfruit. The overlapped curves are boundaries of the original and, with −70% scaling, −50% scaling, +50% scaling and +70% scaling.

overlap for all shape categories. Hence, it can also be concluded that this method is highly invariant to size of starfruits.

The system was also tested for starfruit samples with blemishes and other types of mechanical injuries. Blemish textures is usually translated to the formation of black or darker bands especially along the longitudinal ridges of starfruits. For this type of blemishes, the surface light reflectance was relatively lower than a normal surface, shifting towards darker region or low hue values. Tests showed that some starfruits with blemishes could still accurately be classified for both shape and colour. It was discovered, however, that changing the lighting intensity levels during inspection affects the results of classification. Although in theory hue should be independent of the intensity of an image, experiments showed that hue histogram of starfruits changes with the changing of intensity levels. Therefore, it is critical to ensure that the intensity level remains the same for both sample training and testing stages.

6. Conclusions

The algorithm have successfully been developed for quality control inspection of starfruits using machine vision application. Both the linear discriminant analysis and multi-layer preceptron neural network have been investigated for colour mapping of starfruits. Testings have been performed using all features from hue 10 to 74 and using selected hues produced by Wilks-lambda analysis. Results indicated that DA have recorded a significant improvement when selected features were used, producing an average success rate of better than 95% during testing process. The same trend was not observed for MLP. This method resulted in the average correct classification of slightly better than 90% during training or testing process. The method of feature reduction via Wilks-lambda technique seems effective for DA but not for MLP.

Starfruit shapes could be discriminated using method based on the Fourier descriptor. Shape information have been extracted and compressed from the normalised boundary and Fourier transform. The angle code histogram technique was incorporated in the thinning algorithm, making this technique of shape separation invariant to rotations and scalings. A shape separator based on fourth, fifth and sixth-order harmonics have been defined, and the machine grading have demonstrated a 100% agreement with professional human inspector. The above methods and procedures could, therefore, provide a reliable building blocks for developing an overall automated inspection system that would be beneficial to starfruits industry in promoting grading consistency and standardisation.

Acknowledgments

MZA acknowledges the support of the Malaysia Ministry of Science, Technology and Innovation through the award of research grant in the Intensified Research in Priority Area (grant number 60101813). The authors would like to thank Federal Agricultural Malaysia Authority for useful discussions.

References

Abdullah, M. Z., Aziz, S. A., & Mohamed, A. M. D. (2000). Quality inspection of bakery product using a color-based machine vision system. *Journal of Food Quality, 23*(1), 39–50.

Abdullah, M. Z., Guan, L. C., & Mohd-Azemi, B. M. N. (2001). Stepwise discriminant analysis for colour grading of oil palm using machine vision system. *Transaction of the IChemE, 79*(C), 223–231.

Aleixos, N., Blasco, J., Navarron, F., & Molto, E. (2002). Multispectra inspection of citrus in real-time using machine vision and digital processors. *Computers and Electronics in Agriculture, 33*(2), 121–137.

Baruch, O., & Luew, M. H. (1988). Segmentation of two-dimensional boundaries using the chain code. *Pattern Recognition, 21*(6), 581–589.

Celenk, M. (1990). A colour clustering technique for image segmentation. *Computer Vision, Graphics and Image Processing, 52*, 145–170.

Dillon, W. R., & Goldstein, M. (1984). *Multivariate analysis methods and applications*. New York, USA: John Wiley & Sons.

Du, C. J., & Sun, D. W. (2004). Recent developments in the applications of image processing techniques for food quality evaluation. *Trends in Food Science and Technology, 15*(5), 230–249.

Fahlman, S. E., & Lebiere, C. (1990). The cascade-correlation learning architecture. In D. S. Touretzky (Ed.). *Advances in neural information processing systems* (Vol. 2, pp. 524–532). California, USA: Morgan Kaufmann Publisher.

Gombar, V. K., & Enslein, K. (1991). A structure biodegradability relationship model by discriminant analysis. In J. Devillers & W. Karcher (Eds.), *Chemical environmental science studies* (pp. 377–414). The Netherlands: Academic Publishers.

Haykin, S. (1999). *Neural networks: A comprehensive foundation*. London, UK: Macmillan College.

Heinemann, P. H., Hughes, R., Morrow, C. T., Sommer, H. J., III, Beelman, R. B., & Wuest, P. J. (1994). Grading of mushrooms using machine vision system. *Transactions of the ASAE, 37*(5), 1671–1677.

Heinemann, P. H., Pathare, N. P., & Morrow, C. T. (1996). An automated inspection station for machine vision grading of potatoes. *Machine Vision and Applications, 9*, 14–19.

Heinemann, P. H., Varghese, Z. A., Morrow, C. T., Sommer, H. J., III, & Crasweller, R. M. (1995). Machine vision inspection of golden delicious apples. *Transactions of the ASAE, 11*(6), 901–906.

Kader, A. A. (1999). Fruit maturity, ripening, and quality relationships. *Acta Horticulture, 485*, 203–208.

Lee, S. K., & Kader, A. A. (2000). Preharvest and postharvest factors influencing vitamin C content of horticulture crops. *Postharvest Biology and Technology, 20*, 207–220.

MacKay, D. J. C. (1992). Bayesian interpolation. *Neural Computation, 4*, 415–447.

McConnel, R. K. & Blau, H. H. (1995). Color classification of non-uniform baked and roasted foods. *FPAC IV conference*, Chicago, USA.

Mitcham, F. J., & McDonald, R. E. (1991). Characterization of the ripening of carambola (*Averrhoa carambola* L.) fruit. *Proceedings Florida State Horticulture Society, 104*, 104–108.

Morrison, D. F. (1967). *Multivariate statistical analysis*. New York, USA: McGraw-Hill.

Nakasone, H. Y., & Paull, R. R. (1998). *Tropical fruits*. Wallingford, UK: CAB International.

Paliwal, Y., Shashidhar, N. S., & Jayas, D. S. (1999). Grain kernel identification using kernel signature. *Transactions of the ASAE, 42*(6), 1921–1924.

Peng, H. L., & Chen, S. Y. (1997). Trademark shape recognition using closed contours. *Pattern Recognition Letter, 18*, 791–803.

Rahman, M. A., & Johari, S. (1992). Genetic variety. In M. A. Rahman, A. Izham, & M. L. Raziah (Eds.), *Guidelines of starfruits production* (pp. 9–12). Malaysia: Malaysia Agricultural Research Development Institute (MARDI).

Rencher, A. C., & Larson, S. F. (1980). Bias in Wilks-lambda in stepwise discriminant analysis. *Technometrics, 22*(3), 349–356.

Shearer, S. A., & Payne, F. A. (1990). Color and defect sorting of bell peppers using machine vision. *Transactions of the ASAE, 33*(6), 2045–2050.

Smith, M. A., & Nakai, S. (1990). Classification of cheese by multivariate analysis of HPLC profiles. *Canadian Institute of Food Science and Technology Journal, 23*, 53–58.

Tao, Y., Morrow, C. T., Heinemann, P. H., & Sommer, H. J. III, (1995). Fourier based separation technique for shape grading of potatoes using machine vision. *Transactions of the ASAE, 38*(3), 949–957.

Zahn, C. T., & Rookies, R. Z. (1972). Fourier descriptors for plane closed curves. *IEEE Transaction of Computers, C*(21), 269–281.